

# Event Stream-based Sign Language Translation: A High-Definition Benchmark Dataset and A Novel Baseline

Shiao Wang<sup>1</sup>, Xiao Wang<sup>1\*</sup>, Duoqing Yang<sup>1</sup>, Yao Rong<sup>1</sup>, Fuling Wang<sup>1</sup>, Jianing Li<sup>2</sup>, Lin Zhu<sup>3</sup>, Bo Jiang<sup>1</sup>

<sup>1</sup>School of Computer Science and Technology, Anhui University, Hefei, China

<sup>2</sup>Qiyuan Laboratory, Beijing, China

<sup>3</sup>Beijing Institute of Technology, Beijing, China

*e24101001@stu.ahu.edu.cn, xiaowang@ahu.edu.cn, e125221163@stu.ahu.edu.cn,*

*rytaptap@163.com, e23201049@stu.ahu.edu.cn, ,*

*linzhu@pku.edu.cn, jiangbo@ahu.edu.cn*

## Abstract

*Sign Language Translation (SLT) is a core task in the field of AI-assisted disability. Traditional SLT methods are typically based on visible light videos, which are easily affected by factors such as lighting variations, rapid hand movements, and privacy concerns. This paper proposes the use of bio-inspired event cameras to alleviate the aforementioned issues. Specifically, we introduce a new high-definition event-based sign language dataset, termed Event-CSL, which effectively addresses the data scarcity in this research area. The dataset comprises 14,827 videos, 14,821 glosses, and 2,544 Chinese words in the text vocabulary. These samples are collected across diverse indoor and outdoor scenes, covering multiple viewpoints, lighting conditions, and camera motions. We have also benchmarked existing mainstream SLT methods on this dataset to facilitate fair comparisons in future research. Furthermore, we propose a novel event-based sign language translation framework, termed EvSLT. The framework first segments continuous video features into clips and employs a Mamba-based memory aggregation module to compress and aggregate spatial detail features at the clip level. Subsequently, these spatial features, along with temporal representations obtained from temporal convolution, are then fused by a graph-guided spatiotemporal fusion module. Extensive experiments on Event-CSL, as well as other publicly available datasets, demonstrate the superior performance of our method. The dataset and source code will be released on <https://github.com/Event-AHU/OpenESL>*

## 1. Introduction

With the rapid development of deep learning, AI (*Artificial Intelligence*) for good has received widespread attention, among which, Sign Language Translation (SLT) [43, 45, 47] is increasingly being emphasized. It facilitates communication between deaf individuals and non-signers by translating sign language videos into natural language text, thereby significantly enhancing social participation and quality of life for the deaf community. However, the performance of sign language translation is still limited due to the usage of traditional RGB cameras, as it is easily influenced by limited frame rate, illumination, motion blur, etc. In addition, the deployment of RGB-based sign language translation models raises potential ethical concerns, as it inherently involves issues related to human privacy.

Recently, biologically inspired event cameras (e.g., DVS346, Prophesee, CeleX) have drawn more and more attention due to their unique advantages in *high dynamic range, low energy cost, sparse spatial but dense temporal resolution, and low latency*, etc. [7]. In terms of the imaging mechanism, each pixel in an event camera operates independently and asynchronously, which fundamentally differs from RGB cameras that capture synchronized frame-based outputs. A binary pulse signal is recorded only when the change in brightness for each pixel exceeds a specific threshold. Some computer vision tasks have involved the event camera for event-based or event-enhanced learning, such as object detection [8], tracking [33, 36], action recognition [37, 39], and also the sign language translation [46] discussed in this paper.

Although research in this area remains limited, several studies have recently begun to explore event-based sign language translation (SLT) and sign language recognition (SLR), as illustrated in Fig. 1. Early approaches are typically developed using simulated event data generated from

\*✉ Corresponding Author: Xiao Wang

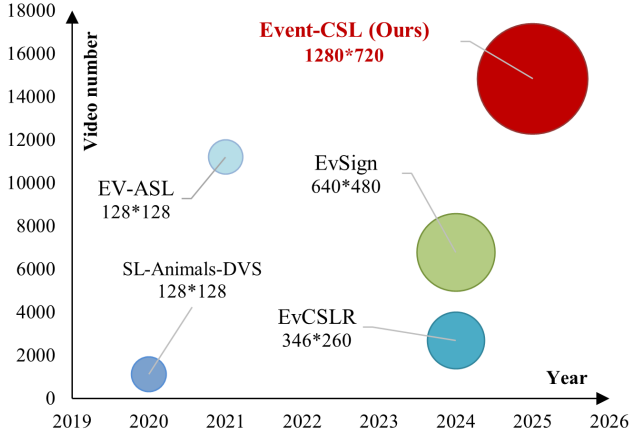


Figure 1. Comparison between existing event-based sign language datasets and our newly proposed Event-CSL benchmark dataset. The bubble size represents the resolution.

existing RGB datasets, such as PHOENIX-2014 [17] and CSL-Daily [48]. However, such simulated data fail to fully capture the essential characteristics of real event streams. Recently, four real event-based datasets have been introduced, namely SL-Animal-DVS [31], EV-ASL [40], EvCSLR [14], and EvSign [46]. The first three datasets are designed for the SLR task and suffer from low spatial resolutions ( $128 \times 128$  and  $346 \times 260$ ), while EvSign [46] removes the actors’ head regions for privacy protection. We argue that this operation may distort the event signals, thereby negatively impacting the recognition and analysis of gestures involving head movements. In addition, to reduce the substantial computational complexity introduced by spatial modeling, most existing SLT methods [46, 47] primarily focus on temporal modeling, while overlooking the crucial role of spatial detail features in gesture understanding.

In this paper, we propose a new sign language translation dataset, termed Event-CSL, which is the largest, high-definition ( $1280 \times 720$ ) real-event dataset collected using the Prophesee EVK4-HD event camera. It contains 14,827 videos, 14,821 glosses, and 2,544 Chinese words in the text vocabulary. Our dataset is collected across diverse indoor and outdoor scenes, covering multiple viewpoints, lighting conditions, and camera motions. More importantly, we provide the most primitive event stream data, which lays the groundwork for accurately recognizing the meanings conveyed by gestures. In our experiments, we split these videos into training, validation, and testing subsets, which contain 12,602, 741, and 1,484 samples, respectively. To build a more comprehensive benchmark, we retrain and evaluate recently released SLT models for future work to compare. More details can be found in Section 4.

Based on the newly proposed Event-CSL dataset, we further propose a novel event-based sign language trans-

lation framework, termed EvSLT. As shown in Fig. 2, we first feed the event video frames into a visual encoder, which is composed of residual networks [11], to extract visual features. The resulting video features are then segmented into consecutive video clip features of a predefined length, following the temporal order of the frames. Features from these fixed-length video clip are subsequently compressed and aggregated using a Mamba-based memory aggregation module to capture fine-grained spatial details. Together with temporal features extracted via an average pooling layer and temporal convolution, the compressed clip features and aggregated spatial features are fed into a graph-guided spatiotemporal fusion module, where hypergraphs constructed from the compressed clip features serve as a bridge to enable effective interactions between spatial and temporal representations. Finally, the spatiotemporally fused features are projected into language model embedding space through a sign embedding layer, and then fed into a language model (mBART [24]) for decoding into sign language text.

To sum up, the main contributions of this paper can be summarized as the following three aspects:

- 1). We propose a new large-scale, high-definition event-based sign language translation dataset, termed Event-CSL. It contains 14,827 videos, 14,821 glosses, and 2,544 Chinese words recorded in both indoor and outdoor scenarios.
- 2). We propose a novel event-based sign language translation framework, termed EvSLT. It employs a Mamba-based memory aggregation module to compress and aggregate spatial features, and introduces a graph-guided spatiotemporal fusion module for spatiotemporal interaction.
- 3). Extensive experiments conducted on two event-based SLT datasets, i.e., EvSign, and our Event-CSL, fully validated the effectiveness of our framework.

## 2. Related Work

### 2.1. Sign Language Translation

Sign language translation (SLT) aims to transform sign language videos into spoken text, thereby facilitating communication for deaf individuals. In earlier years, Camgöz et al. [2] introduced the SLT task. Traditional gloss-based methods [3, 6, 43] first translate sign language videos into glosses and then convert those glosses into spoken text. Joint-SLT [3] proposes a Transformer-based framework that jointly learns continuous sign language recognition and translation in an end-to-end manner. Recently, gloss-free SLT methods [22, 41, 45, 47] have gained increasing attention for removing the need for costly gloss annotations. For example, Zhou et al. [47] propose a two-stage approach, which bridges the semantic gap between visual and text representation and restores masking sentences. Sign2GPT [41] leverages LLM for gloss-free sign language translation.

Different from previous works, we explore an event-based, gloss-free SLT task, leveraging the high dynamic range, high temporal resolution, and inherent privacy benefits of event cameras to enable accurate and reliable translation.

## 2.2. State Space Model

State space models (SSMs) [16] have recently gained attention due to their linear complexity. Gu et al. [10] propose the Structured State Space sequence model, which reparameterizes the SSM, stabilizes the state matrix via low-rank correction, and simplifies computation through a Cauchy kernel formulation. Mamba [9] is a sequence modeling approach with linear complexity that addresses the low computational efficiency of traditional methods on long sequences. In computer vision, VMamba [25] extends the visual Mamba with four-directional scanning while retaining the benefits of a global receptive field and dynamic weights. Vim [49] further introduces a bidirectional vision Mamba block that serves as a universal backbone for vision tasks. Following the design of vision Mamba, many recent visual models [13, 19, 29, 42] adopt similar strategies to achieve efficient spatial modeling. Building upon these advances, this paper employs the vision Mamba block to aggregate spatial details from video clips, thereby effectively enhancing sign language translation performance.

## 3. Methodology

### 3.1. Overview

As illustrated in Fig. 2, we propose a unified framework for event-based sign language translation. Input event streams are first stacked into event frames and passed through a visual encoder to extract features. Temporal dynamics are modeled using average pooling followed by temporal convolution, while a Mamba-based memory aggregation module compresses and aggregates clip-level spatial representations. A graph-guided spatiotemporal fusion module then constructs relational graphs from the compressed clip features, enabling effective interaction between enhanced spatial details and temporal dependencies. Finally, the fused spatiotemporal features are projected via a sign embedding module and decoded by a language model (mBART [24]) to generate accurate Chinese sentences.

### 3.2. Input Representation

Given event streams  $\mathcal{E}^p = \{e_1, e_2, \dots, e_M\}$ , where  $M$  denotes the number of event points, each point  $e_i | i \in (1, M)$  is a quadruple  $\{x, y, t, p\}$ , here the  $(x, y)$  denotes the spatial coordinates,  $t$  and  $p$  denotes the time stamp and polarity, respectively. To make full use of existing deep neural networks, we first stack the event streams of each video into a sequence of event frames, denoted as  $\mathcal{E}^T = \{E_1, E_2, \dots, E_T\}$ , where  $T$  denotes the number of

stacked frames. Each event frame is then resized to a fixed resolution, i.e.,  $E_i \in \mathbb{R}^{C \times H \times W}$ . Here,  $\{C, H, W\}$  denotes the dimensions of the channel, height, and width of an event frame, respectively. During training, we randomly sample a mini-batch of  $B$  event video samples as input, with dimensions  $B \times T \times C \times H \times W$ .

### 3.3. Network Architecture

• **Visual Encoder and Temporal Branch.** Given an input of size  $B \times T \times C \times H \times W$ , we first employ a residual network as the visual encoder to extract visual feature representations for video frames. Specifically, we reshape the input by merging the batch and temporal dimensions into  $B \times T \rightarrow B * T$ , resulting in a tensor of size  $B * T \times C \times H \times W$ , and then fed into ResNet-18 [11] to extract visual features, yielding video feature maps  $\mathbf{F} \in \mathbb{R}^{B \times T \times C' \times H' \times W'}$  ( $H' = H/32, W' = W/32$ ). Here,  $C', H'$ , and  $W'$  denote the channel dimension, height, and width of the feature maps obtained after the hierarchical downsampling of ResNet-18.

In the temporal branch, we perform global average pooling over the spatial dimensions of the extracted feature maps to obtain the temporal features  $\mathbf{F}_t \in \mathbb{R}^{B \times T \times C'}$ . After that, we employ two temporal convolution blocks to aggregate temporal information and obtain the aggregated temporal features  $\mathbf{F}'_t \in \mathbb{R}^{B \times T' \times C'}$ . It can be formulated as:

$$\begin{aligned} \mathbf{H}^{(1)} &= \text{MaxPool} \left( \sigma \left( \text{BN} \left( \text{Conv1d}_5^{(1)} \left( \mathbf{F}_t \right) \right) \right) \right), \\ \mathbf{F}'_t &= \text{MaxPool} \left( \sigma \left( \text{BN} \left( \text{Conv1d}_5^{(2)} \left( \mathbf{H}^{(1)} \right) \right) \right) \right), \end{aligned} \quad (1)$$

where  $\text{Conv1d}_5^{(i)}(\cdot)$  denotes the 1D convolution with kernel size 5 in the  $i$ -th temporal convolution block,  $\text{MaxPool}$  represents the max pooling operation, and  $\sigma(\cdot)$  denotes the ReLU activation function. Temporal convolution enables the model to capture continuous hand movements and establish coherent temporal dependencies, thereby improving contextual understanding and translation accuracy.

• **Mamba-based Memory Aggregation.** To preserve spatial detail while reducing computational cost, we introduce a Mamba-based memory aggregation module to compress and aggregate spatial features. Specifically, we first divide the continuous video features  $\mathbf{F} \in \mathbb{R}^{B \times T \times C' \times H' \times W'}$  into fixed-length video clip features along the temporal dimension, resulting in  $n$  clip features, denoted as  $\mathbf{F}_c = \{\mathbf{F}_c^1, \mathbf{F}_c^2, \dots, \mathbf{F}_c^n\}$ . Consequently, the spatial feature of each video clip can be represented as  $\mathbf{F}_c^i \in \mathbb{R}^{B \times \frac{T}{n} \times C' \times H' \times W'}$ , which can be further reshaped into  $\mathbf{F}_c^i \in \mathbb{R}^{B \times \frac{T \cdot H' \cdot W'}{n} \times C'}$ . Next, we apply global average pooling to the spatial feature of the  $i$ -th video clip to compress them and obtain a compressed clip feature representation  $\mathbf{F}_g^i \in \mathbb{R}^{B \times 1 \times C'}$ . The resulting compressed clip feature is then concatenated with the spatial features of the corre-

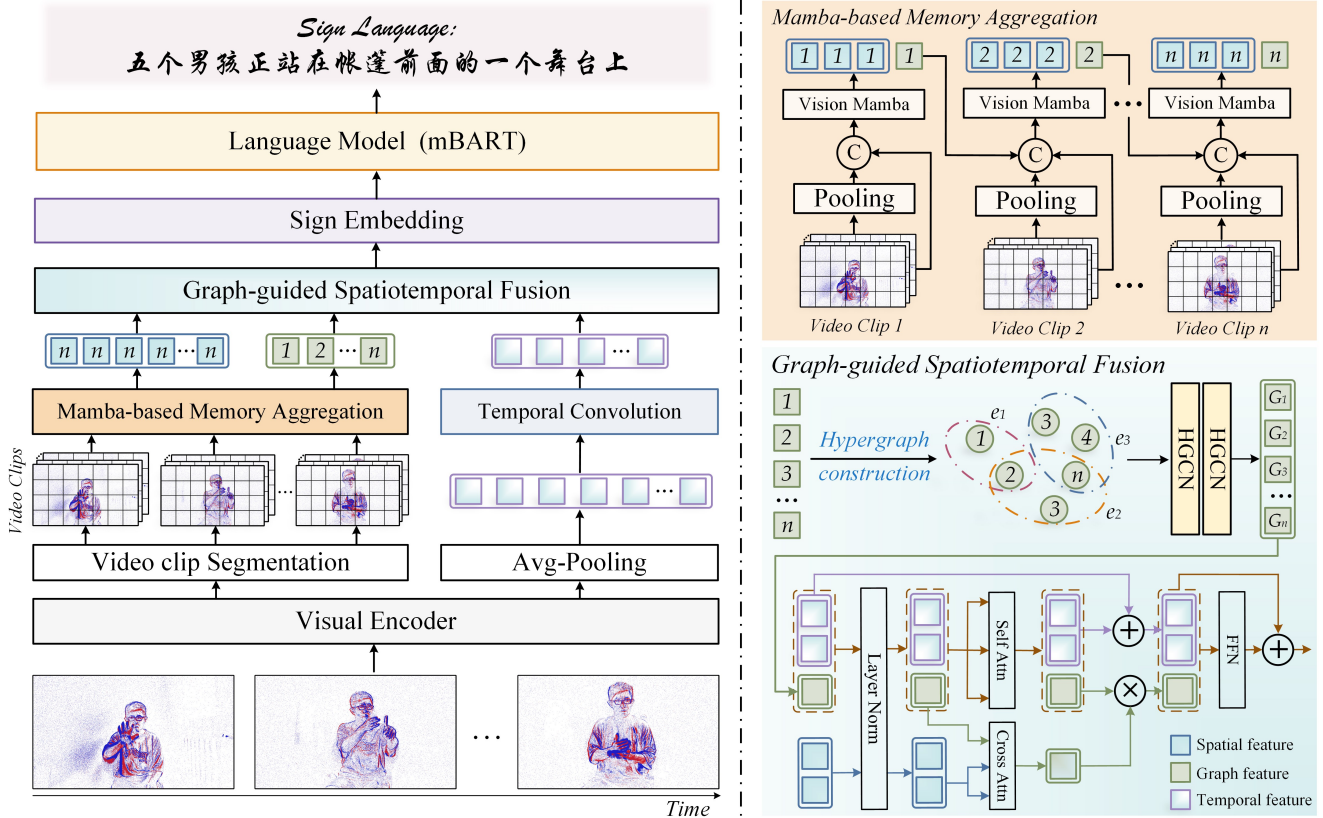


Figure 2. **An overview of the proposed event-based sign language translation framework.** The framework segments continuous video features into clip features and employs a Mamba-based memory aggregation module to compress and aggregate spatial details. The resulting spatial and compressed clip features, together with temporal representations from temporal convolution, are fused in a graph-guided spatiotemporal fusion module. Hypergraphs built from compressed clip features facilitate interaction between memory-enhanced spatial and temporal representations. Finally, a Transformer-based language model generates the corresponding Chinese sentences.

sponding video clip and fed into the visual Mamba network for spatial feature aggregation.

Following vision Mamba [49], the concatenated vision features are first normalized through a normalization layer, and then projected into features  $x$  and  $z$  using two linear layers. Specifically, we also employ both forward and backward scanning to process the input. For each direction, we obtain  $x'$  using the 1D convolution layer and SiLU activation function:

$$x' = \text{SiLU}(\text{Conv}(x)). \quad (2)$$

After that, the output  $x'$  is projected to yield the input matrix  $\mathbf{B} \in \mathbb{R}^{N \times T}$ , output matrix  $\mathbf{C} \in \mathbb{R}^{T \times N}$ , and also the timescale parameter  $\Delta$ :

$$\mathbf{B}, \mathbf{C}, \Delta = \text{Linear}(x'), \quad (3)$$

Here, the timescale parameter  $\Delta$  is used for discretization, as the raw SSM is designed for a continuous system, but the data we process are discretized visual tokens. The Zero-

Order Hold (ZOH) rule is adopted to discretize the continuous state space matrices:

$$\overline{\mathbf{A}}, \overline{\mathbf{B}} = \text{ZOH}(\mathbf{A}, \mathbf{B}, \Delta), \quad (4)$$

where  $\mathbf{A} \in \mathbb{R}^{N \times N}$  is the state matrix. Therefore, the formula of the discretized SSM can be denoted as:

$$h' = \overline{\mathbf{A}}h + \overline{\mathbf{B}}x', \quad y = \mathbf{C}h', \quad (5)$$

where  $h$  and  $h'$  represent the hidden state,  $x'$  and  $y$  are the inputs and output. The forward and backward SSM branches are applied for bidirectional context awareness to produce  $y_{for}$ ,  $y_{back}$ . After that,  $y_{for}$ ,  $y_{back}$  are gated by  $z$  and the result of their addition is linearly projected to  $y'$ , which can be written as:

$$y' = \text{Linear}(y_{for} \odot \text{SiLU}(z) + y_{back} \odot \text{SiLU}(z)). \quad (6)$$

For each video clip feature  $\mathbf{F}_c^i$ , we apply the aforementioned series of operations, and the resulting compressed

clip features  $\mathbf{F}_g^{(i)'}$  are pass to the  $(i + 1)$ -th video clip feature to enable inter-clip information exchange and memory aggregation. Mathematically, this can be expressed as:

$$\mathbf{F}_g^{(i+1)'}, \mathbf{F}_c^{(i+1)'} = \text{Mamba}([\mathbf{F}_g^{(i)'}, \mathbf{F}_g^{i+1}, \mathbf{F}_c^{i+1}]), \quad (7)$$

where  $[\cdot]$  denotes concatenation, and the compressed feature of the previous clip is discarded.

In this way, we progressively aggregate the detailed spatial features of each clip in a forward manner, analogous to how the human brain sequentially remember each video clip from beginning to end, resulting in the final aggregated spatial features  $\mathbf{F}_s = \mathbf{F}_c^{(n)'}$  along with the compressed clip features  $\mathbf{F}_g = [\mathbf{F}_g^{(1)'}, \mathbf{F}_g^{(2)'}, \dots, \mathbf{F}_g^{(n)'}]$ . Next, the memory-enhanced spatial features  $\mathbf{F}_s$ , the compressed clip features  $\mathbf{F}_g$ , and the temporal features  $\mathbf{F}'_t$  are jointly fed into the graph-guided spatiotemporal fusion module.

• **Graph-guided Spatiotemporal Fusion.** To capture the complex relationships among different video clips, we treat the compressed feature vectors of video clips as nodes to construct hypergraphs. Following [5], we adopt K-nearest neighbors (K-NN, where the maximum number of neighboring nodes is set to 10 in our work) based on Euclidean distance to generate the hypergraph structure  $\mathcal{H}$ . It can be formulated as:

$$\mathcal{H} = \{V, \mathcal{E}, \mathbf{H}\},$$

$$\text{where } \mathbf{H}_{ji} = \begin{cases} 1, & \text{if } v_j \in e_i, \\ 0, & \text{otherwise,} \end{cases} \quad (8)$$

$$\mathbf{G} = \mathbf{D}_v^{-\frac{1}{2}} \mathbf{H} \mathbf{D}_e^{-1} \mathbf{H}^\top \mathbf{D}_v^{-\frac{1}{2}}, \quad (9)$$

where  $\mathbf{H}$  is the node–hyperedge incidence matrix,  $V$  and  $\mathcal{E}$  denote the vertex and hyperedge set.  $\mathbf{D}_v$  and  $\mathbf{D}_e$  are the node degree matrix and hyperedge degree matrix, respectively.  $\mathbf{G}$  denotes the normalized hypergraph propagation matrix. Subsequently, we feed  $\mathbf{G}$  into Hypergraph Convolutional Network (HGCN) [5] to facilitate effective interaction among video clips:

$$\mathbf{X}' = \mathbf{G}(\mathbf{X}\mathbf{W} + \mathbf{b}), \quad (10)$$

where the  $\mathbf{X}$  and  $\mathbf{X}'$  denote the input and output feature vectors, i.e.,  $\mathbf{F}_g$  and  $\mathbf{F}'_g$ , respectively.  $\mathbf{W}$  is the learnable weight matrix and  $\mathbf{b}$  is the bias.

To enable effective interaction between spatial and temporal features, i.e.,  $\mathbf{F}_s$  and  $\mathbf{F}'_t$ , we propose to use graph features  $\mathbf{F}'_g$  derived from the compressed clip representations as a bridge to enable efficient spatiotemporal interaction. Specifically, we first pass the spatial, temporal, and graph features through a shared layer normalization layer. This is followed by two parallel attention networks that process

the features concurrently. Let  $SA$  and  $CA$  denote the self-attention and cross-attention mechanisms, respectively. The temporal and graph features are concatenated and input to the  $SA$  module, whereas the graph and spatial features serve as the query and context, respectively, for the  $CA$  module. It can be expressed by the following formulas:

$$\begin{aligned} [\mathbf{F}_t^{\text{SA}}, \mathbf{F}_g^{\text{SA}}] &= \text{SA}([\mathbf{F}'_t, \mathbf{F}'_g]), \\ \mathbf{F}_g^{\text{CA}} &= \text{CA}(\mathbf{F}'_g, \mathbf{F}_s), \end{aligned} \quad (11)$$

where the  $\mathbf{F}_g^{\text{SA}}$  and  $\mathbf{F}_g^{\text{CA}}$  denote the output graph features of  $SA$  and  $CA$ , respectively. Subsequently, the two attention-enhanced graph features are combined via element-wise multiplication, together with the  $SA$ -enhanced temporal features, fed into a feedforward neural network. The feedforward network aggregates and transforms the attention-enhanced features, producing the final spatiotemporally enhanced fused representation. Since the detailed spatial features consist of a large number of tokens, whereas the temporal and graph features contain relatively few, this design provides two key advantages. First, the graph features act as a bridge, facilitating effective interactions between the spatial and temporal features. Second, it substantially reduces the computational burden of the attention mechanism, since the spatial detail features are only used as the keys and values in the cross-attention operation.

• **Sign Language Decoder.** Once the spatiotemporally enhanced features are obtained, they are fed into a sign embedding module, which consists of a linear layer and a ReLU activation. Finally, a language decoder is adapted to generate sign language sentences. In our practical implementation, we use the pre-trained parameters of *mBART* [24] to initialize the language model, which consists of 3 Transformer encoder layers and 3 Transformer decoder layers. Note that we directly output the language based on given input event streams, without the help of gloss annotations, i.e., our model is a gloss-free SLT framework.

### 3.4. Loss Function

The language decoder sequentially generates the logits of sign language sentence  $S$ , which can be expressed as:

$$S = \{p(\langle \text{bos} \rangle), p(w_1), p(w_2), \dots, p(w_U), p(\langle \text{eos} \rangle)\}. \quad (12)$$

The first special word  $\langle \text{bos} \rangle$  marks the beginning of the sentence, the last special word  $\langle \text{eos} \rangle$  marks the end of the sentence, and  $p(w)$  represents the logits of the generated words. In this work, we adopt the widely used *cross-entropy loss* function to calculate the distance between the annotated sign language sentence and the generated sentence, which can be formulated as:

$$\mathcal{L} = -\log \prod_{u=1}^U p(s_u | w_u). \quad (13)$$

Table 1. Comparison of the datasets for sign language recognition and translation.

Dataset	Year	Language	#Videos	Resolution	Gloss	Text	Source	Raw Data	Scene	Continuous	SLT	Event
SIGNUM [32]	2010	DGS	15,075	776 × 578	455	-	Lab	-	-	✓	✗	✗
DEVISIGN-G [4]	2015	CSL	432	640 × 480	36	-	Lab	-	-	✗	✗	✗
DEVISIGN-D [4]	2015	CSL	6,000	640 × 480	500	-	Lab	-	-	✗	✗	✗
DEVISIGN-L [4]	2015	CSL	24,000	640 × 480	2,000	-	Lab	-	-	✗	✗	✗
PHOENIX-2014 [17]	2015	DGS	6,841	210 × 260	1,081	-	TV	-	-	✓	✗	✗
PHOENIX-2014T [2]	2018	DGS	8,257	210 × 260	1,066	2,887	TV	-	-	✓	✓	✗
MSASL [15]	2018	ASL	25,513	-	1,000	-	Web	-	-	✗	✗	✗
INCLUDE [30]	2020	ISL	4,287	1920 × 1080	263	-	Lab	-	-	✗	✗	✗
CSL-Daily [48]	2021	CSL	20,654	1920 × 1080	2,000	2,343	Lab	-	-	✓	✓	✗
SL-Animals-DVS [31]	2020	SSL	1,121	128 × 128	19	-	Lab	✓	Indoor	✗	✗	✓
EV-ASL [40]	2021	ASL	11,200	128 × 128	56	-	Lab	-	-	✗	✗	✓
EvCSLR [14]	2024	CSL	2,685	346 × 260	423	-	Lab	✓	Indoor	✓	✗	✓
EvSign [46]	2024	CSL	6,773	640 × 480	1,387	1,947	Lab	✓	Indoor	✓	✓	✓
Event-CSL (Ours)	2025	CSL	<b>14,827</b>	<b>1280 × 720</b>	<b>14,821</b>	<b>2,544</b>	Lab	✓	Indoor, Outdoor	✓	✓	✓

## 4. Event-CSL Dataset

### 4.1. Protocols

When collecting our sign language translation dataset Event-CSL, we follow the following protocols: 1). *Diversity of views*: We capture different perspectives of sign language, including slightly downward, horizontal, and slightly upward views. 2). *Camera motions*: Our dataset collection takes into account a variety of motion patterns, including fast movement, slow movement, and moderate movement. 3). *Diversity of scenes*: In order to conform to the daily use of sign language, we consider different usage scenarios when recording videos. Specifically, these scenarios comprise office environments, daily life, and outdoor scenes (such as streets, parking lots, and open spaces). 4). *Intensity of light*: In environments with strong or weak light intensity (high and low exposure), event cameras can still record information about the movement of objects due to the presence of pixel changes. We record videos under different lighting conditions, including strong, low, and dim light. 5). *Continuity of action*: Keep the movement of sign language flowing and coherent when recording sign language, reducing useless information and redundant video frames. 6). *Diversity of sign language content*: To better reflect real-world applications, sign language videos should cover diverse content. We randomly extract captions from the COCO-CN [20] dataset, encompassing daily life, outdoor activities, animals and plants, sports, character introductions, and landscapes.

### 4.2. Statistical Analysis

Our proposed dataset is the first large-scale, high-definition event-based sign language benchmark. All videos are recorded using the Prophesee EVK4-HD event camera at a resolution of 1280 × 720. In total, the dataset contains 14,827 sign language videos, 14,821 gloss annotations, and a vocabulary of 2,544 Chinese words. We randomly divide the dataset into training, validation, and test sets with

12,602, 741, and 1,484 videos, respectively. The text corpus includes sentences ranging from 8 to 75 characters, with an average length of 18. As shown in Table 1, our dataset significantly surpasses existing event-based sign language datasets in terms of video quantity, spatial resolution, gloss annotations, and vocabulary diversity. The representative samples from Event-CSL with their corresponding text annotations are illustrated in Fig. 3, and the word-cloud visualization is shown in Fig. 5.

### 4.3. Benchmark Baselines

To construct a comprehensive benchmark dataset for event-based sign language translation, we retrain and report the performance of the following sign language translation algorithms as the baselines on the Event-CSL dataset for future works to compare: 1). **Gloss-based SLT**: Joint-SLT [3], Chen et al. [6], Sign-XmDA [43]; 2). **Gloss-free SLT**: TSPNet [18], GASLT [45], GFSLT [47], SignCL [44], Sign2GPT [41], and Wang et al. [34].

## 5. Experiment

### 5.1. Dataset and Evaluation Metric

Our experiments are conducted on four event-based sign language translation datasets, including the newly proposed **Event-CSL**, and public **EvSign** [46], **PHOENIX-2014T-Event** [2], **CSL-Daily-Event** [48] datasets.

- **EvSign Dataset** [46] is an event-based sign language dataset collected from daily-life scenarios, including social interactions, education, shopping, travel, and healthcare. It is recorded by multiple sign language volunteers, and its annotations are extracted and reorganized from the National Sign Language Dictionary of China and CSL-Daily to form fluent oral sentences. The training, validation, and testing sets contain 5,570, 553, and 650 sign language videos, respectively. In total, EvSign includes 1,387 Chinese glosses and a vocabulary of 1,947 Chinese words.

- **PHOENIX-2014T-Event Dataset** [2] is derived from

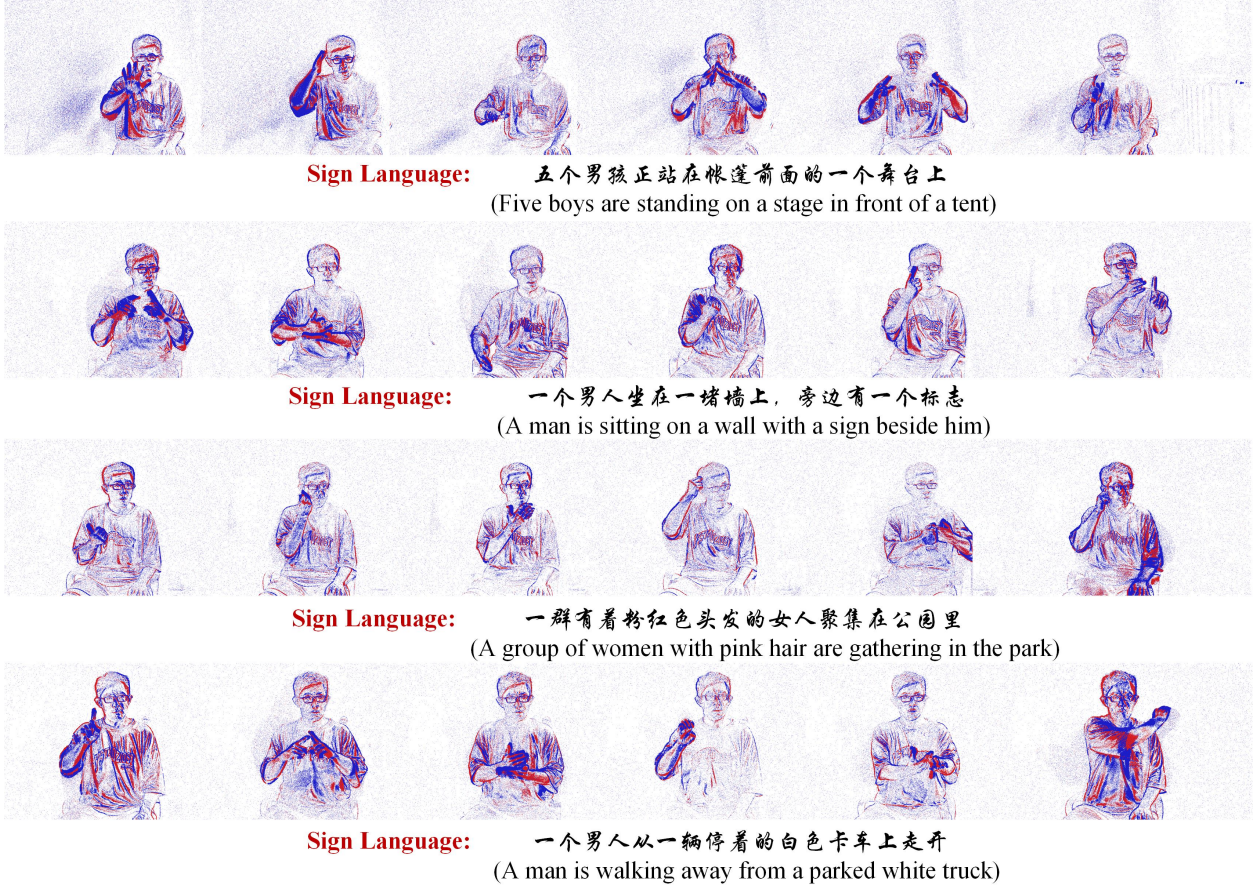


Figure 3. Representative samples from our proposed Event-CSL dataset and the corresponding text annotations

Table 2. Experimental results on our Event-CSL dataset.

No.	Algorithm	Publish	Backbone	ROUGE	BLEU-1	BLEU-2	BLEU-3	BLEU-4
01	Joint-SLT [3]	CVPR2020	ViT	27.76	30.30	19.15	12.63	8.99
02	Chen et al. [6]	CVPR2022	S3D	23.15	24.35	13.93	8.01	5.11
03	Sign-XmdA [43]	ArXiv2023	ViT	31.48	34.60	23.56	16.62	12.39
04	GASLT [45]	CVPR2023	ViT	31.69	34.27	23.41	16.73	12.64
05	TSPNet [18]	NeurIPS2020	I3D	26.63	30.91	17.84	10.89	7.25
06	GFSLT [47]	ICCV2023	CNN	67.23	69.00	60.62	53.77	48.20
07	SignCL [44]	NeurIPS2024	CNN	67.76	69.12	60.88	54.18	48.52
08	Wang et al. [34]	ArXiv2024	CNN, Mamba	68.02	69.71	61.35	54.40	48.70
09	Sign2GPT [41]	ICLR2024	ViT	68.74	70.35	61.98	55.13	49.23
10	Ours	-	CNN	<b>68.93</b>	<b>70.40</b>	<b>62.09</b>	<b>55.34</b>	<b>49.80</b>

German Sign Language weather broadcast videos. The original PHOENIX-2014T dataset consists of RGB video frames captured by conventional cameras. To generate an event-based version, we use DVS-Voltmeter [23], a stochastic process-based event simulator for dynamic vision sensors, as illustrated in Fig. 4(a). We denote the resulting event representation as PHOENIX-2014T-Event, which preserves the same dataset configuration as PHOENIX-

2014T in terms of the number of videos and German annotations. The training, validation, and testing sets contain 7,096, 519, and 642 sign language videos, respectively. In total, the PHOENIX-2014T-Event dataset includes 1,066 German glosses and a vocabulary of 2,887 German words.

- **CSL-Daily-Event Dataset [48]** is derived from daily life scenarios, covering multiple themes such as family life, healthcare, and school life. We also obtain its event rep-

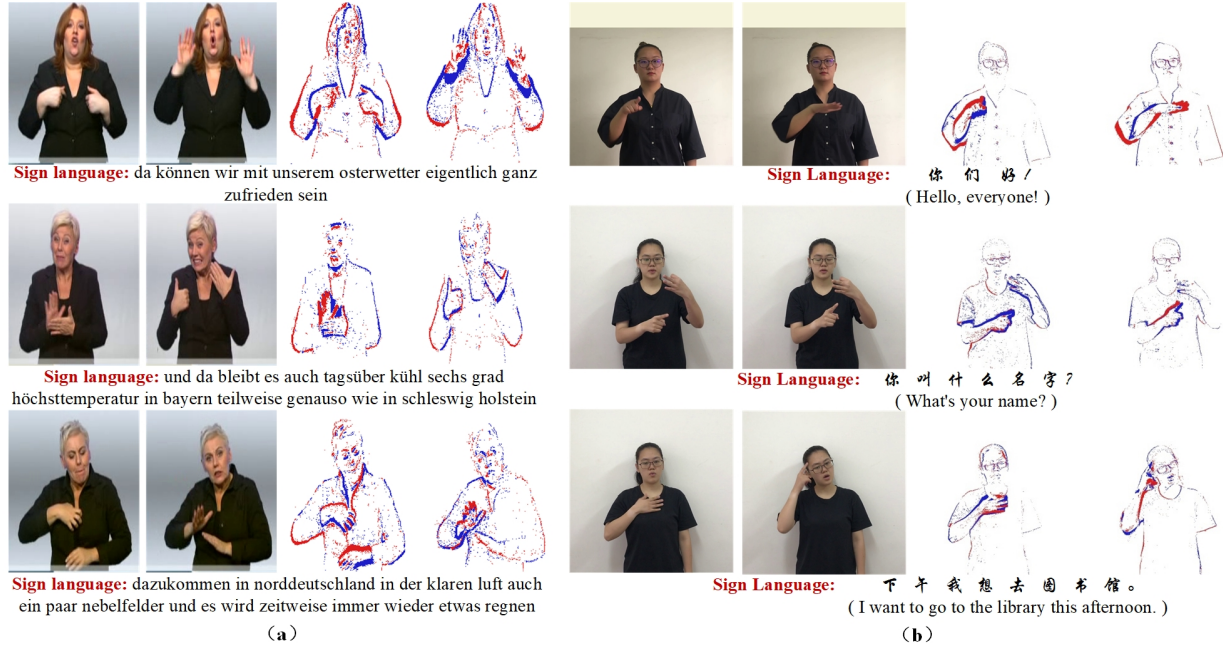


Figure 4. The samples of video frames on the PHOENIX-2014T and CSL-Daily simulation datasets

Table 3. Comparison between our model and other SOTA algorithms on the EvSign dataset.

No.	Algorithm	Publish	Backbone	Modality	ROUGE	BLEU-1	BLEU-2	BLEU-3	BLEU-4
01	Joint-SLT [3]	CVPR2020	ViT	RGB	40.05	39.84	23.54	15.60	10.63
02	VAC+TH [26]	ICCV2021	CNN,BiLSTM	RGB	39.08	38.74	23.90	15.88	10.19
03	CorrNet+TH [12]	CVPR2023	CNN,BiLSTM	RGB	39.41	39.45	23.74	15.68	10.57
04	Joint-SLT [3]	CVPR2020	ViT	Event	41.54	40.13	24.36	16.04	10.87
05	VAC+TH [26]	ICCV2021	CNN,BiLSTM	Event	39.48	39.22	24.11	15.94	10.01
06	CorrNet+TH [12]	CVPR2023	CNN,BiLSTM	Event	41.23	40.85	25.34	16.95	11.83
07	GFSLT [47]	ICCV2023	CNN	Event	51.98	54.26	35.91	24.97	17.88
08	Zhang et al. [46]	ECCV2024	CNN,BiLSTM,ViT	Event	42.43	41.44	25.61	17.55	12.37
09	Ours	-	CNN	Event	<b>53.43</b>	<b>55.45</b>	<b>38.45</b>	<b>27.41</b>	<b>20.20</b>

Table 4. Comparison between our model and other SOTA algorithms on the PHOENIX-2014T-Event dataset.

No.	Algorithm	Publish	Backbone	ROUGE	BLEU-1	BLEU-2	BLEU-3	BLEU-4
01	TSPNet [18]	NeurIPS2020	I3D	18.16	19.41	8.61	5.92	4.67
02	Joint-SLT [3]	CVPR2020	ViT	20.80	21.25	13.60	9.96	7.89
03	Sign-XmDA [43]	ArXiv2023	ViT	24.21	24.80	16.24	11.91	9.36
04	GASLT [45]	CVPR2023	ViT	24.94	25.81	17.00	12.47	9.82
05	GFSLT [47]	ICCV2023	CNN	33.45	34.66	24.63	18.49	14.72
06	Ours	-	CNN	<b>34.98</b>	<b>35.60</b>	<b>25.98</b>	<b>20.18</b>	<b>16.48</b>

Table 5. Comparison between our model and other SOTA algorithms on the CSL-Daily-Event dataset.

No.	Algorithm	Publish	Backbone	ROUGE	BLEU-1	BLEU-2	BLEU-3	BLEU-4
01	TSPNet [18]	NIPS2020	I3D	10.01	10.69	4.43	2.36	1.45
02	Joint-SLT [3]	CVPR2020	ViT	12.68	13.47	6.63	3.79	2.44
03	Sign-XmDA [43]	ArXiv2023	ViT	13.84	14.50	7.75	4.50	2.87
04	GASLT [45]	CVPR2023	ViT	15.25	14.42	8.48	5.20	3.39
05	GFSLT [47]	ICCV2023	CNN	20.81	20.82	13.42	8.98	6.37
06	Ours	-	CNN	<b>27.06</b>	<b>27.14</b>	<b>15.68</b>	<b>10.13</b>	<b>7.09</b>



method surpasses it by +10.77% and +7.12% in ROUGE-L and BLEU-4, respectively, without leveraging any sign language gloss annotations. Compared with GFSLT, our model achieves additional improvements of +1.53% and +1.76% on the ROUGE-L and BLEU-4 metrics, respectively. These experiments further demonstrate the generalization ability of our method on this dataset.

• **Results on CSL-Daily-Event Dataset.** As shown in Table 5, we report the results on the simulated CSL-Daily-Event dataset. For the gloss-based methods, our method improves by +13.22% and +4.22%, respectively, in ROUGE-L and BLEU-4 compared to Sign-XmDA. For the gloss-free methods, our method improves by +6.25% and +0.72%, respectively, compared to GFSLT. The results of these experiments demonstrate that our method can also achieve good performance on the event simulation dataset.

#### 5.4. Ablation Study

• **Component Analysis on Event-CSL.** To demonstrate the effectiveness of our method, we evaluate the contribution of each module on the Event-CSL dataset, as shown in Table 6. We first compare the temporal and spatial branches, and find that temporal features outperform spatial ones by a large margin, as sign language translation relies heavily on temporal continuity. Combining spatial details with temporal representations allows the model to better capture fine-grained motion and contextual cues. We then examine the impact of the Mamba layer in the spatial branch. Replacing it with simple MLPs results in a 0.6% drop in accuracy, confirming the benefit of the Mamba-based design. Finally, the fourth experiment validates the contribution of the proposed Graph-guided Spatiotemporal Fusion (GSTF) module. Overall, these results demonstrate the effectiveness of all components in our framework.

• **Analysis of the Number of Input Event Frames.** The number of input frames in sign language videos significantly affects both the model’s performance and its computational resource usage. To investigate this, we set four different frame sampling ratios: L/8, L/4, L/2, and L, where L denotes the total number of frames in each sign language video. As shown in Table 7, we compare the model’s performance under these four frame settings on the Event-CSL dataset. The results demonstrate that as the number of frames increases, the model performance consistently improves. When all the video frames (L) are used, the performance is several times higher than that obtained using only L/8 frames. This indicates that increasing the number of input event frames enriches the temporal context, which in turn improves translation quality.

• **Analysis of Different Resolutions of Event Frames.** As shown in Table 7, we conducted experiments using four different input resolutions for event frames:  $112 \times 112$ ,  $224 \times 224$ ,  $256 \times 256$ , and  $320 \times 320$ . It can be ob-

Table 7. Analysis of **Input Frames**, **Input Resolutions**, and **Different Spatiotemporal Fusion Methods**. R represents ROUGE-L, and B-1, B-2, B-3, B-4 represent BLEU-1, BLEU-2, BLEU-3, and BLEU-4, respectively.

# Input Frames	R	B-1	B-2	B-3	B-4
L / 8	29.93	33.36	22.01	14.89	10.62
L / 4	48.26	50.20	40.37	33.23	27.92
L / 2	59.69	61.67	52.52	45.44	39.80
L	<b>68.93</b>	<b>70.40</b>	<b>62.09</b>	<b>55.34</b>	<b>49.80</b>
# Input Resolutions	R	B-1	B-2	B-3	B-4
$112 \times 112$	48.04	50.12	42.16	36.28	31.72
$256 \times 256$	68.52	69.96	61.54	54.67	49.06
$320 \times 320$	68.88	70.38	62.03	55.24	49.68
$224 \times 224$	<b>68.93</b>	<b>70.40</b>	<b>62.09</b>	<b>55.34</b>	<b>49.80</b>
Fusion Methods	R	B-1	B-2	B-3	B-4
Concatenate	65.79	67.32	59.09	52.43	47.00
Cross-Attention	67.65	69.27	60.76	53.98	48.84
Ours w/o Graph	68.81	69.82	61.45	54.65	49.07
Ours (GSTF)	<b>68.93</b>	<b>70.40</b>	<b>62.09</b>	<b>55.34</b>	<b>49.80</b>

Table 8. Efficiency Analysis on Event-CSL dataset.

Algorithm	# Params	# FLOPs	# Speed
SignCL [44]	115.5M	266.5G	175 ms/video
Sign2GPT [41]	1771.1M	490.5G	247 ms/video
EvSLT (Ours)	138.2M	252.0G	86 ms/video

served that the best performance is achieved at a resolution of  $224 \times 224$ . Larger resolutions, on the other hand, lead to performance degradation. We attribute this to the fact that high-resolution event inputs often introduce more redundant noise, and existing models are not yet well adapted to high-resolution event data. Nevertheless, we believe that high-definition event cameras still hold great potential in scenarios requiring detailed contour capture or larger receptive fields for tracking fast-moving targets. Existing high-resolution event datasets, such as EventVOT [36], EvDET200K [38], and Celex-HAR [35], together with our proposed Event-CSL, will contribute to advancing research in this community.

• **Analysis of Different Spatiotemporal Fusion Methods.** The graph-guided spatiotemporal fusion (GSTF) module is a key component of our framework. In Table 7, we compare it with other feature-level fusion methods. The results show that our spatiotemporal fusion approach outperforms alternative fusion strategies. Moreover, when the hypergraph modeling strategy is removed (Ours w/o Graph), the performance drops significantly, demonstrating the effectiveness of using a hypergraph to capture relationships between video clips.

• **Analysis of the Depth of Mamba Network.** As shown in Fig. 6 (a), we compare the effect of different numbers of Mamba layers on the final performance. The results show

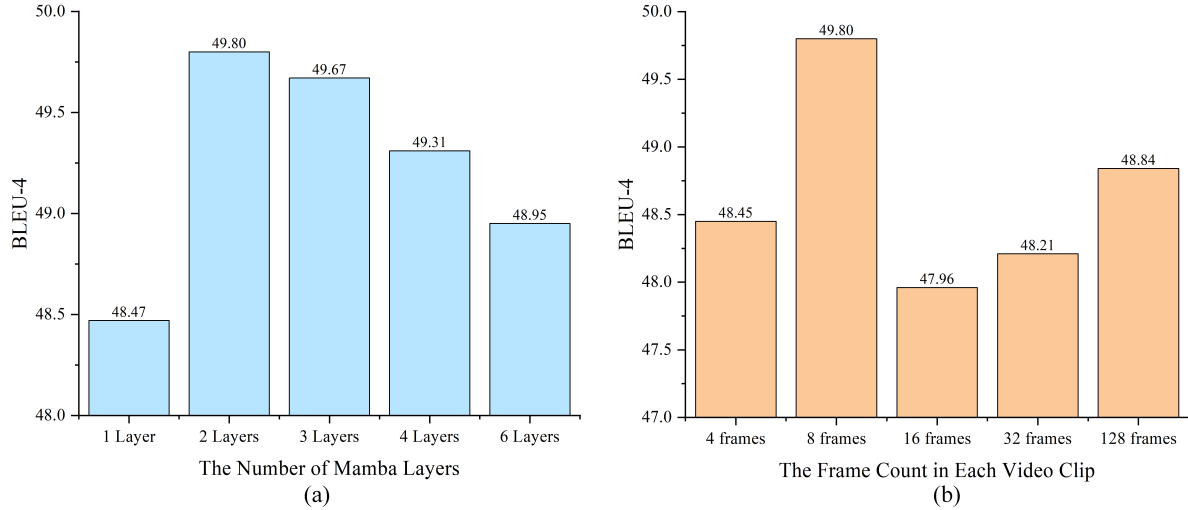


Figure 6. (a) Comparison with different numbers of Mamba layers. (b) Comparison with different frame counts in each video clip.

	<p><b>Reference:</b> 几个孩子和他们的两只黑色狗在小山上玩耍 (Several children and their two black dogs are playing on the hill)</p> <p><b>Ours:</b> 几个孩子和他们的两只黑色狗在小山上玩耍</p> <p><b>Ours w/o Spatial:</b> 几个孩子和他们的黑狗在小山上玩耍</p>
	<p><b>Reference:</b> 一个女人站在雨中，拿着一把伞和一个毛绒玩具 (A woman is standing in the rain, holding an umbrella and a plush toy)</p> <p><b>Ours:</b> 一个女人站在雨中，拿着一把伞和一只绒毛玩具</p> <p><b>Ours w/o Spatial:</b> 一个女人站在雨中，拿着一把伞和一个绒动物</p>
	<p><b>Reference:</b> 在一个阳光灿烂的日子里，两个女人骑自行车 (On a sunny day, two women ride bicycles)</p> <p><b>Ours:</b> 在一个阳光灿烂的日子里，两个女人骑自行车</p> <p><b>Ours w/o Spatial:</b> 在一个阳光灿烂的日子里，两个人骑着自行车</p>
	<p><b>Reference:</b> 一位留着胡子的男士坐在他的卡车门口 (A bearded man is sitting in front of his truck)</p> <p><b>Ours:</b> 一位留着胡须的男士坐在他的大卡车门口</p> <p><b>Ours w/o Spatial:</b> 一位留着胡须的男士坐在他的客门口</p>

Figure 7. A qualitative comparison of the generated sign language translation texts.

that two stacked Mamba layers yield the optimal configuration. When only a single Mamba layer is used, the model accuracy decreases by 1.33%, indicating that the model has limited capacity to capture the complex spatiotemporal dependencies across video clips. In contrast, further increasing the number of Mamba layers also leads to performance degradation. Therefore, a two-layer Mamba provides a good trade-off between accuracy and efficiency, resulting in the best overall performance.

• **Analysis of the Frame Count in Each Video Clip.** As shown in Fig. 6 (b), we analyze the number of frames contained in each video clip of the Event-CSL dataset. It can be observed that both too few and too many frames result

in performance degradation. When the number of frames is too small, the model receives insufficient contextual information to capture the complete motion dynamics and contextual semantics of sign language. In contrast, an excessive number of frames introduces redundant or irrelevant visual information, increasing the model’s learning burden and even leading to overfitting. Therefore, we choose to include a fixed number of 8 frames per video clip to achieve the best performance.

## 5.5. Efficiency Analysis

Table 6 presents a component-wise performance analysis and the associated model parameters. The results show that

our framework achieves notable performance gains with only a marginal increase in model parameters. By integrating spatial feature aggregation and spatiotemporal fusion, it achieves a balanced trade-off between complexity and accuracy. Furthermore, as shown in Table 8, we compare our model with recent methods on parameters, FLOPs, and speed. Our model maintains low computational cost and delivers the fastest translation speed (approximately 86 ms per video). Notably, our method utilizes a unified single-stage framework, achieving higher translation accuracy while remaining computationally efficient.

## 5.6. Visualization

In this section, we present a qualitative analysis of the sign language translation results. As shown in the Fig. 7, **Reference** denotes the ground-truth translation sentence corresponding to the video, **Ours** represents the translation result generated by our model, and **Ours w/o spatial** indicates the result obtained using only the temporal branch, without spatial detail features. The red text highlights incorrectly translated keywords, while the green text shows the correct translations of those keywords. It can be observed that, after removing spatial detail features, the model loses its ability to perceive and translate fine-grained sign details, e.g., “两只黑色狗 (two black dogs)” instead of simply “黑狗 (black dog)”. This demonstrates that our proposed spatiotemporal fusion method effectively enhances the model’s ability to translate detailed components.

## 6. Limitation Analysis

Although our newly proposed SLT framework works well on multiple benchmark datasets, we believe this model can still be improved in the following aspects: 1). We transform the event streams into event frames and resize them into  $224 \times 224$ . Designing novel architectures to better leverage high-definition event data remains an interesting direction for future research. 2). We adopt a relatively lightweight language model (mBART) for sign language generation due to the limited computational resources. We believe a larger language model can bring us a much better performance. We leave these two issues as our future work.

## 7. Conclusion

In this paper, we propose Event-CSL, the first large-scale, high-definition sign language translation dataset captured using an event camera, aiming to bridge the data scarcity gap in this field. The dataset consists of 14,827 high-definition sign language videos with a resolution of  $1280 \times 720$ , along with 14,821 glosses and 2,544 Chinese words in the text vocabulary. We believe that Event-CSL will serve as a valuable resource for advancing research in event-based sign language translation. Furthermore, we

propose a unified spatiotemporal fusion framework for the sign language translation task. To enhance spatial detail representation, we first introduce a Mamba-based memory aggregation module to compress and aggregate video clip features. Then, a graph-guided spatiotemporal fusion module leverages the compressed clip features as a bridge to effectively fuse spatial features with temporal representations, enabling more precise capture of sign language details. We hope that the proposed dataset and model will contribute to the advancement of this field and enable deaf individuals to communicate more freely.

## References

- [1] Léon Bottou. Stochastic gradient descent tricks. In *Neural Networks: Tricks of the Trade: Second Edition*, pages 421–436. Springer, 2012.
- [2] Necati Cihan Camgoz, Simon Hadfield, Oscar Koller, Hermann Ney, and Richard Bowden. Neural sign language translation. In *Proceedings of the IEEE conference on computer vision and pattern recognition*, pages 7784–7793, 2018.
- [3] Necati Cihan Camgoz, Oscar Koller, Simon Hadfield, and Richard Bowden. Sign language transformers: Joint end-to-end sign language recognition and translation. In *Proceedings of the IEEE/CVF conference on computer vision and pattern recognition*, pages 10023–10033, 2020.
- [4] X Chai, H Wanga, M Zhou, G Wub, H Lic, and X Chena. Devisign: dataset and evaluation for 3d sign language recognition. *Technical report, Beijing, Tech. Rep*, 2015.
- [5] Ines Chami, Rex Ying, Christopher Ré, and Jure Leskovec. Hyperbolic graph convolutional neural networks. *Advances in neural information processing systems*, 32:4869, 2019.
- [6] Yutong Chen, Fangyun Wei, Xiao Sun, Zhirong Wu, and Stephen Lin. A simple multi-modality transfer learning baseline for sign language translation. In *Proceedings of the IEEE/CVF conference on computer vision and pattern recognition*, pages 5120–5130, 2022.
- [7] Guillermo Gallego, Tobi Delbrück, Garrick Orchard, Chiara Bartolozzi, Brian Taba, Andrea Censi, Stefan Leutenegger, Andrew J Davison, Jörg Conradt, Kostas Daniilidis, et al. Event-based vision: A survey. *IEEE transactions on pattern analysis and machine intelligence*, 44(1):154–180, 2020.
- [8] Daniel Gehrig and Davide Scaramuzza. Low-latency automotive vision with event cameras. *Nature*, 629(8014):1034–1040, 2024.
- [9] Albert Gu and Tri Dao. Mamba: Linear-time sequence modeling with selective state spaces. *CoRR*, abs/2312.00752, 2023.
- [10] Albert Gu, Karan Goel, and Christopher Ré. Efficiently modeling long sequences with structured state spaces. In *International Conference on Learning Representations*, 2021.
- [11] Kaiming He, Xiangyu Zhang, Shaoqing Ren, and Jian Sun. Deep residual learning for image recognition. In *Proceedings of the IEEE Conference on Computer Vision and Pattern Recognition (CVPR)*, 2016.
- [12] Lianyu Hu, Liqing Gao, Zekang Liu, and Wei Feng. Continuous sign language recognition with correlation network.

- In *Proceedings of the IEEE/CVF Conference on Computer Vision and Pattern Recognition*, pages 2529–2539, 2023.
- [13] Ju Huang, Shiao Wang, Shuai Wang, Zhe Wu, Xiao Wang, and Bo Jiang. Mamba-fetrack: Frame-event tracking via state space model. In *Chinese Conference on Pattern Recognition and Computer Vision (PRCV)*, pages 3–18. Springer, 2024.
- [14] Yu Jiang, Yuehang Wang, Siqi Li, Yongji Zhang, Qianren Guo, Qi Chu, and Yue Gao. Evcslr: Event-guided continuous sign language recognition and benchmark. *IEEE Transactions on Multimedia*, 2024.
- [15] Hamid Reza Vaezi Joze and Oscar Koller. Ms-asl: A large-scale data set and benchmark for understanding american sign language. In *British Machine Vision Conference*, page 100, 2018.
- [16] Rudolph Emil Kalman. A new approach to linear filtering and prediction problems. 1960.
- [17] Oscar Koller, Jens Forster, and Hermann Ney. Continuous sign language recognition: Towards large vocabulary statistical recognition systems handling multiple signers. *Computer Vision and Image Understanding*, 141(1):108–125, 2015.
- [18] Dongxu Li, Chenchen Xu, Xin Yu, Kaihao Zhang, Benjamin Swift, Hanna Suominen, and Hongdong Li. Tspnet: Hierarchical feature learning via temporal semantic pyramid for sign language translation. *Advances in Neural Information Processing Systems*, 33:12034–12045, 2020.
- [19] Kunchang Li, Xinhao Li, Yi Wang, Yanan He, Yali Wang, Limin Wang, and Yu Qiao. Videomamba: State space model for efficient video understanding. In *European conference on computer vision*, pages 237–255. Springer, 2024.
- [20] Xirong Li, Chaoxi Xu, Xiaoxu Wang, Weiyu Lan, Zhengxiong Jia, Gang Yang, and Jieping Xu. Coco-cn for cross-lingual image tagging, captioning and retrieval. *IEEE Transactions on Multimedia*, 21(9):2347–2360, 2019.
- [21] Chin-Yew Lin. Rouge: A package for automatic evaluation of summaries. In *Text summarization branches out*, pages 74–81, 2004.
- [22] Kezhou Lin, Xiaohan Wang, Linchao Zhu, Ke Sun, Bang Zhang, and Yi Yang. Gloss-free end-to-end sign language translation. In *Annual Meeting of the Association for Computational Linguistics*, 2023.
- [23] SongNan Lin, Ye Ma, Zhenhua Guo, and Bihan Wen. Dvs-voltmeter: Stochastic process-based event simulator for dynamic vision sensors. *European Conference on Computer Vision*, 13667:578–593, 2022.
- [24] Yinhan Liu, Jiatao Gu, Naman Goyal, Xian Li, Sergey Edunov, Marjan Ghazvininejad, Michael Lewis, and Luke Zettlemoyer. Multilingual denoising pre-training for neural machine translation. *Transactions of the Association for Computational Linguistics*, 8:726–742, 2020.
- [25] Yue Liu, Yunjie Tian, Yuzhong Zhao, Hongtian Yu, Lingxi Xie, Yaowei Wang, Qixiang Ye, and Yunfan Liu. Vmamba: Visual state space model. *CoRR*, abs/2401.10166, 2024.
- [26] Yuecong Min, Aiming Hao, Xiujuan Chai, and Xilin Chen. Visual alignment constraint for continuous sign language recognition. In *Proceedings of the IEEE/CVF international conference on computer vision*, pages 11542–11551, 2021.
- [27] Kishore Papineni, Salim Roukos, Todd Ward, and Wei-Jing Zhu. Bleu: a method for automatic evaluation of machine translation. In *Proceedings of the 40th annual meeting of the Association for Computational Linguistics*, pages 311–318, 2002.
- [28] Adam Paszke, Sam Gross, Francisco Massa, Adam Lerer, James Bradbury, Gregory Chanan, Trevor Killeen, Zeming Lin, Natalia Gimelshein, Luca Antiga, et al. Pytorch: An imperative style, high-performance deep learning library. *Advances in neural information processing systems*, 32, 2019.
- [29] Yuan Shi, Bin Xia, Xiaoyu Jin, Xing Wang, Tianyu Zhao, Xin Xia, Xuefeng Xiao, and Wenming Yang. Vmambair: Visual state space model for image restoration. *IEEE Transactions on Circuits and Systems for Video Technology*, 2025.
- [30] Advait Sridhar, Rohith Gandhi Ganesan, Pratyush Kumar, and Mitesh Khapra. Include: A large scale dataset for indian sign language recognition. In *ACM International Conference on Multimedia*, pages 1366–1375, 2020.
- [31] Ajay Vasudevan, Pablo Negri, Bernabe Linares-Barranco, and Teresa Serrano-Gotarredona. Introduction and analysis of an event-based sign language dataset. In *2020 15th IEEE International Conference on Automatic Face and Gesture Recognition (FG 2020)*, pages 675–682. IEEE, 2020.
- [32] Ulrich von Agris and Karl-Friedrich Kraiss. Signum database: Video corpus for signer-independent continuous sign language recognition. In *4th Workshop on the Representation and Processing of Sign Languages: Corpora and Sign Language Technologies*, pages 243–246, 2010.
- [33] Xiao Wang, Jianing Li, Lin Zhu, Zhipeng Zhang, Zhe Chen, Xin Li, Yaowei Wang, Yonghong Tian, and Feng Wu. Vi-sevent: Reliable object tracking via collaboration of frame and event flows. *IEEE transactions on cybernetics*, 54(3):1997–2010, 2024.
- [34] Xiao Wang, Yao Rong, Fuling Wang, Jianing Li, Lin Zhu, Bo Jiang, and Yaowei Wang. Event stream based sign language translation: A high-definition benchmark dataset and a new algorithm. *arXiv preprint arXiv:2408.10488*, 2024.
- [35] Xiao Wang, Shiao Wang, Pengpeng Shao, Bo Jiang, Lin Zhu, and Yonghong Tian. Event stream based human action recognition: a high-definition benchmark dataset and algorithms. *arXiv preprint arXiv:2408.09764*, 2024.
- [36] Xiao Wang, Shiao Wang, Chuanming Tang, Lin Zhu, Bo Jiang, Yonghong Tian, and Jin Tang. Event stream-based visual object tracking: A high-resolution benchmark dataset and a novel baseline. In *Proceedings of the IEEE/CVF Conference on Computer Vision and Pattern Recognition*, pages 19248–19257, 2024.
- [37] Xiao Wang, Zongzhen Wu, Bo Jiang, Zhimin Bao, Lin Zhu, Guoqi Li, Yaowei Wang, and Yonghong Tian. Hardvs: Revisiting human activity recognition with dynamic vision sensors. In *Proceedings of the AAAI Conference on Artificial Intelligence*, pages 5615–5623, 2024.
- [38] Xiao Wang, Yu Jin, Wentao Wu, Wei Zhang, Lin Zhu, Bo Jiang, and Yonghong Tian. Object detection using event camera: A moe heat conduction based detector and a new benchmark dataset. In *Proceedings of the Computer Vision and Pattern Recognition Conference*, pages 29321–29330, 2025.

- [39] Yanxiang Wang, Xian Zhang, Yiran Shen, Bowen Du, Guangrong Zhao, Lizhen Cui, and Hongkai Wen. Event-stream representation for human gaits identification using deep neural networks. *IEEE Transactions on Pattern Analysis and Machine Intelligence*, 44(7):3436–3449, 2021.
- [40] Yong Wang, Xian Zhang, Yanxiang Wang, Hongbin Wang, Chanying Huang, and Yiran Shen. Event-based american sign language recognition using dynamic vision sensor. In *Workshop on Applications of Software Agents*, pages 3–10, 2021.
- [41] Ryan Wong, Necati Cihan Camgoz, and Richard Bowden. Sign2GPT: Leveraging large language models for gloss-free sign language translation. In *The Twelfth International Conference on Learning Representations*, 2024.
- [42] Yijun Yang, Zhaohu Xing, Lequan Yu, Chunwang Huang, Huazhu Fu, and Lei Zhu. Vivim: A video vision mamba for medical video segmentation. *arXiv preprint arXiv:2401.14168*, 2024.
- [43] Jinhui Ye, Wenxiang Jiao, Xing Wang, Zhaopeng Tu, and Hui Xiong. Cross-modality data augmentation for end-to-end sign language translation. *arXiv preprint arXiv:2305.11096*, 2023.
- [44] Jinhui Ye, Xing Wang, Wenxiang Jiao, Junwei Liang, and Hui Xiong. Improving gloss-free sign language translation by reducing representation density. *Advances in Neural Information Processing Systems*, 37:107379–107402, 2024.
- [45] Aoxiong Yin, Tianyun Zhong, Li Tang, WeiKe Jin, Tao Jin, and Zhou Zhao. Gloss attention for gloss-free sign language translation. In *Proceedings of the IEEE/CVF Conference on Computer Vision and Pattern Recognition*, pages 2551–2562, 2023.
- [46] Pengyu Zhang, Hao Yin, Zeren Wang, Wenyue Chen, Shengming Li, Dong Wang, Huchuan Lu, et al. Evsign: Sign language recognition and translation with streaming events. *ECCV*, 2024.
- [47] Benjia Zhou, Zhigang Chen, Albert Clapés, Jun Wan, Yanyan Liang, Sergio Escalera, Zhen Lei, and Du Zhang. Gloss-free sign language translation: Improving from visual-language pretraining. In *Proceedings of the IEEE/CVF International Conference on Computer Vision (ICCV)*, pages 20871–20881, 2023.
- [48] Hao Zhou, Wengang Zhou, Weizhen Qi, Junfu Pu, and Houqiang Li. Improving sign language translation with monolingual data by sign back-translation. In *Proceedings of the IEEE/CVF Conference on Computer Vision and Pattern Recognition*, pages 1316–1325, 2021.
- [49] Lianghui Zhu, Bencheng Liao, Qian Zhang, Xinlong Wang, Wenyu Liu, and Xinggang Wang. Vision mamba: Efficient visual representation learning with bidirectional state space model. *Computing Research Repository*, abs/2401.09417, 2024.